Rigothier, C. C., Saleem, M. A., Bourget, C., Mathieson, P. W., Combe, C., & Welsh, G. I. (2016). Nuclear translocation of IQGAP1 protein upon exposure to puromycin aminonucleoside in cultured human podocytes: ERK pathway involvement. *Cellular Signalling*, *28*(10), 1470-1478. https://doi.org/10.1016/j.cellsig.2016.06.017

Nuclear translocation of IQGAP1 protein upon exposure to puromycin aminonucleoside in cultured human podocytes: ERK pathway involvement

Claire Rigothier [1, 2, 3], Moin Ahson Saleem [1, 4], Chantal Bourget [2], Peter William Mathieson [1], Christian Combe [2, 3], and Gavin Iain Welsh [1].

[1] Bristol Renal, University of Bristol, Bristol, United Kingdom, [2] INSERM U1026, Université de Bordeaux, Bordeaux, France; [3] Service de Néphrologie Transplantation Dialyse, Centre Hospitalier Universitaire de Bordeaux, Bordeaux, France; [4] Children's renal unit, University of Bristol, Bristol, United Kingdom.

Running title: IQGAP1 biology in puromycin model.

Correspondence: Claire RIGOTHIER, Biotis, Unité INSERM U1026, Université de Bordeaux, 33076 Bordeaux, France.

Tel: +33557571488, Fax: +33556900517

E-mail: claire.rigothier@chu-bordeaux.fr

Abstract

IQGAP1, a protein that links the actin cytoskeleton to slit diaphragm proteins, is involved in podocyte motility and permeability. Its regulation in glomerular disease is not known. We have exposed human podocytes to puromycin aminonucleoside (PAN), an inducer of nephrotic syndrome in rats, and studied the effects on IQGAP1 biology and function.

In human podocytes exposed to PAN, a nuclear translocation of IQGAP1 was observed by immunocytolocalization and confirmed by Western blot after selective nuclear/cytoplasmic extraction. In contrast to IQGAP1, IQGAP2 expression remained cytoplasmic. IQGAP1 nuclear translocation was associated with a significant decrease in its interaction with nephrin and podocalyxin. Activation of the ERK pathway was observed in PAN treated podocytes with a preponderant nuclear localization of the phosphorylated form of ERK (P-ERK). The interaction between IQGAP1 and P-ERK increased upon podocyte exposure to PAN. Inhibitors of ERK pathway activation blocked IQGAP1 nuclear translocation ($p<0.02$). Chromatin interaction protein assays demonstrated an interaction of IQGAP1 with chromatin and with Histone H3, which increased in response to PAN.

In summary, PAN induces the ERK dependent translocation of IQGAP1 into the nuclei in human podocytes which leads to the interaction of IQGAP1 with chromatin and Histone H3, and decreased interactions between IQGAP1 and slit-diaphragm proteins. Therefore, IQGAP1 may have a role in podocyte gene regulation in glomerular disease.

Keywords: IQGAP1, nucleus, MAP Kinase pathway, podocytes, slit diaphragm proteins

1. Introduction

In humans, there are two main types of nephrotic syndrome: one due to gene mutations encoding for proteins such as nephrin, podocin, CD2AP, α-actinin-4, TRPC6, PLCε1, INF2 [1-7]; the other type is the idiopathic nephrotic syndrome, which is probably mediated by a circulating factor of lymphocytic origin [8]. Histologic changes that are observed in the two forms are similar with foot process effacement, podocyte swelling, disappearance of the slit diaphragm, actin cytoskeleton redistribution and slit diaphragm protein relocalization. These changes lead to a loss of the glomerular barrier integrity resulting in massive proteinuria.

The scaffold protein IQGAP1 has been shown to interact with nephrin and podocalyxin [9, 10] and also with other components of slit diaphragm complex [11]. We have previously reported the involvement of IQGAP1 in podocyte motility and the permeability of a podocyte monolayer [11] through its role in regulating actin cytoskeleton remodeling and microtubule dynamics [12, 13]. Silencing of IQGAP1 expression reduced podocyte migration ability and increased the permeability of the podocyte layer. This suggests that IQGAP1 may be involved in podocyte structural changes observed in the nephrotic syndrome. Liu et al. recently confirmed this hypothesis: IQGAP1 controlled actin cytoskeleton organization through its interaction with nephrin in a Puromycin AminoNucleoside (PAN) induced nephrotic syndrome in rodents [14].

IQGAP1 belongs to the IQGAP family (proteins with a domain rich in isoleucine -IQ- and RAS GTPase activated relative protein domain without GTPase -GAP-) in which there are three isoforms that have high homology but which have different functions and tissue distributions [15-17]. IQGAP1 is involved in various cell functions through its several interacting domains [15]: proliferation [18-20], cell adhesion [21, 22], exocytosis [23], and gene expression regulation as pro-oncogene [24, 25]. IQGAP1 is also required for the activation and/or functional and biological activities of numerous interacting proteins, including a number of signalling proteins. For example, IQGAP1 binds directly to MEK 1/2

and ERK 1/2 kinases and modulates their activation [26]. It is also a scaffold protein for Ras and Raf, which are both initial elements of the MAP kinase cascade [26, 27]. ERK/MEK activation induces gene transcription through nuclear translocation. MAP kinases are involved, depending of the cell type and the microenvironmental stimuli, in apopotosis, cell survival, proliferation and differentiation.

PAN injection is a recognized model of nephrotic syndrome in rodents [28, 29]. A few days after injection, PAN induces a massive proteinuria due to ultrastructural changes that are similar to those described in human nephrotic syndrome [30-32] In podocytes, the ERK pathway is activated with an increase of ERK phosphorylation upon exposure to puromycin aminonucleoside leading to podocyte apoptosis [32].

In this study we show that exposure of cultured human podocytes to PAN leads to changes in IQGAP1 biology which may be relevant to human disease.

2. Materials and Methods

2.1. Cell culture

The human podocyte cell line, obtained from human nephrectomy specimen without glomerular disease, and the culture conditions have been previously described [33, 34].

2.2. Antibodies

Primary and secondary antibodies used in this study are listed in Table 1.

2.3. PAN and Inhibitor treatments

Podocytes, grown on flaks or coverslips for 14 days, were incubated with 5 µg/ml of PAN (Santa Cruz, Tebu-Bio, Le Perray en Yvelines, France) in serum free medium (RPMI 1640 with penicillin-streptomycin only). After 60 or 90 minutes of exposure to PAN, podocytes

were used for the following experiments. Inhibition of ERK pathway required pre-treatment with the inhibitors: U0126 (10 µM/ml) and/or PD98059 (50 µM/ml), MEK 1/2 and MEK 2 inhibitors respectively (Cell signaling, Ozyme, Saint-Quentin-en-Yvelines, France) 30 minutes before PAN exposure.

2.4. Protein extraction

Total cell extraction required NP40 lysis buffer (Tris 50 mM pH 7,5, NaCl 120 mM, NP40 1%, β-glycerophosphate 40 mM, Benzamidine 1 mM, EDTA 1 mM) with 10 µl/ml protease and phosphatase inhibitor (Sigma, Lyon, France). The suspension was left on ice for 30 min and then centrifuged at 15,000 g. Cytoplasmic and nuclear extracts were obtained using NE-PER cytoplasmic and nuclear extraction reagents® (Pierce, Thermoscientific, Brebières, France) and following manufacturer's instructions. The kit provided efficient cell lysis and extraction of separate cytoplasmic and nuclear protein fractions. Protein quantification was performed on all samples using BCA Protein Assay Reagent (Pierce, Thermoscientific, Brebières, France).

2.5. Western blotting

10 µg of extracted protein were loaded in each well of 7.5, 10 or 15% acrylamide SDS-PAGE gel. WB protocol has been previously described [11] and WB antibodies are summarized in Table 1 and Table 2 for respectively the primary and secondary antibodies. The membranes were visualised using BiochemiHR camera after exposure to SuperSignal West Femto Maximun Sensitivity Substrate (Pierce, Thermoscientific, Brebières, France). Densitometry of signals was performed using the Quantity One software (Bio-Rad, Marnes-la-Coquette, France).

2.6. Quantitative RT-PCR

RT-PCR was performed on total RNA isolated from podocytes. RNA was extracted using trizol. 2 µg of total RNA podocytes were used for the first strand cDNA synthesis with the Superscript™ III first strand synthesis system for RT-PCR (Invitrogen, Cergy Pontoise, France). The primer sequences were: 5'-ATGGCGTTGAAACCACACAG-3' and 5'-TGTGCAGCAACAATCTGA-3'. β-actin was used as standard range. The PCR conditions were 35 cycles with a denaturation 30sec at 95°C, an annealing 30 sec at 60°C and an extension 30 sec at 72°C. qRT-PCR was performed with SYBR green jumpstart Taq Ready Mix (Sigma, Lyon, France).

2.7. Co-immunoprecipitation

Co-immunoprecipitation method have been previously described [11]. 500 µg of proteins were incubated with IQGAP1 polyclonal antibody (3 µg) and 20 µl of protein A/G Agarose beads (Santa Cruz, Tebu-Bio, Le Perray en Yvelines, France). Co-immunoprecipitation with IQGAP1 antibody crosslinked to the beads was used for small proteins. The procedure followed the abcam protocol instructions. During the crosslinking procedure, beads were incubated with IQGAP1 antibody at a concentration of 150 µg/ml. Then, we used 500 µg of proteins incubated with 20 µl of crosslined beads.

2.8. CHIP assay

CHIP assay was performed with control and PAN treated podocytes. Two cell flasks were combined in each condition to obtain a large amount of chromatin. The manufacturer's instructions were followed (Cell signaling, Ozyme, Saint-Quentin-en-Yvelines, France). The amount of antibody used for chromatin immunoprecipitation was respectively 10µl of IQGAP1 and Histone H3 antibodies and 1 µl of rabbit IgG.

2.9. Immunofluorescence

Protocol of immunocytofluorescence (with confocal analysis) have been previously reported [11].

2.10. Statistical analysis

Statistical significance was assessed by appropriate tests with GraphPad® Software (La Jolla, CA). Statistical significance was defined as $p<0.05$.

3. Results

3.1. Nuclear IQGAP1 translocation upon exposure to PAN

Human podocytes were exposed to PAN at a concentration of 5µg/ml for 60 or 90 minutes. Upon exposure to PAN, the subcellular localization of IQGAP1 was analyzed by immunocytofluorescence (Figure 1A). In control cells, IQGAP1 (green labelling) was localized on the plasma membrane, cell contacts and in some instances in the perinuclear area (Control, Figure 1A). Treatment of podocytes with PAN induced a relocalization from its common localization to the nuclei (DAPI or blue labelling, PAN treated cells, Figure 1A) with a persistent IQGAP1 expression at the plasma membrane.

Nuclear translocation of IQGAP1 was confirmed by Western blot analysis (Figure 1B). Western blots were performed on both cytoplasmic and nuclear cell extracts from human podocytes treated for 60 and 90 minutes with PAN: cytoplasmic expression of IQGAP1 decreased upon exposure to PAN, IQGAP1 nuclear expression increased. Lamin A/C and laminin γ1 confirmed differential extraction of the nuclei and the cytoplasm respectively. The ratio between cytoplasmic and nuclear expression, performed after quantification, decreased significantly at 60 and 90 min, demonstrating translocation of IQGAP1 into the nucleus (Figure 1C).

Total protein levels of IQGAP1 remained unchanged upon exposure to PAN. Furthermore, qPCR analysis showed stable transcription levels of IQGAP1 in response to PAN (Supplementary material, Figure S1A to S1C).

Upon exposure to PAN, IQGAP1 phosphorylation increased in total extracts. The phosphorylated form was predominantly and significantly localized in the nuclei. PAN induced an increase in IQGAP1 phosphorylation in subcellular compartments (Data not shown).

3.2. IQGAP2 expression in PAN treated podocytes

Three isoforms have been identified in the IQGAP family with different functions and tissue distributions. IQGAP2 cell localization was analyzed in podocytes under similar conditions to those for IQGAP1. Upon exposure to PAN, IQGAP2 cytoplasmic expression increased and there was a corresponding decrease in nuclear expression (Figure 2A). The cytoplasmic-nuclear ratio revealed a significant cytoplasmic accumulation of IQGAP2 (Figure 2B). In summary, the effect of PAN on IQGAP2 protein was opposite to that observed for IQGAP1.

3.3. Modification of IQGAP1 interaction with podocyte proteins

The expression of podocyte proteins in total cell extracts, nephrin, podocalyxin and α-actinin-4 and the level of phosphorylated nephrin Y1176, remained totally unchanged upon PAN exposure (Supplementary material, Figure S1D). There was no change in their respective cytoplasmic and nuclear localization and expression (Figure 3A) as reflected by graphs of cytoplasmic-nuclear cell extract expression (Figure 3B). NCK 1/2 and MAGI-1 expression in total or cell fractions also remained unchanged between control and PAN conditions (Data not shown).

IQGAP1 is known to interact with podocyte proteins (nephrin and the Y1176 phosphorylated form, podocalyxin, α-actinin-4, NCK 1/2 and MAGI-1). The impact of nuclear IQGAP1

translocation on the level of these interactions was analyzed in both control and PAN treated podocytes. Interaction between IQGAP1 and nephrin decreased significantly at 90 min as did the interaction between IQGAP1 and the phosphorylated form of nephrin and the interaction of IQGAP1 and podocalyxin. There was no change in the interaction between IQGAP1 and the cytoskeleton protein α-actinin-4 (Figure 3C and 3D) or in the interaction between IQGAP1 and NCK 1/2 or MAGI-1 (Data not shown).

3.4. Activation of ERK pathway upon exposure to PAN

The final pathway studied was the ERK pathway, which is known to interact with IQGAP1. PAN treatment resulted in a substantial increase in the phosphorylation of ERK with the most significant effect being seen in the nuclear extract (Figure 4A to 4C). Activation of the ERK pathway was associated with a nuclear translocation of the phosphorylated form, as demonstrated by the decrease of the cytoplasm/nuclei ratio of P-ERK (Figure 4A and 4C). Immunoprecipitation experiments showed a significant increase in the interaction between IQGAP1 and the phosphorylated form of ERK in the nucleus. Interaction between the phosphorylated form and IQGAP1 in the cytoplasmic fraction remained unchanged (Figure 4D and 4E). PAN did not induce a change in the interaction between IQGAP1 and ERK in the total, cytoplasmic or nuclear extracts (Figure 4D and 4E). Interactions between IQGAP1 and ERK or P-ERK in total extracts remained unchanged (Supplementary material, Figure S3).

3.5. Inhibition of nuclear IQGAP1 translocation upon ERK inhibition

These data suggest that PAN induced IQGAP1 nuclear translocation and increased its interaction with P-ERK. To find out if the subcellular relocalization of IQGAP1 required the ERK pathway, we studied whether the translocation of IQGAP1 was affected in the presence of ERK inhibitors.

Podocytes were pretreated for 30 min with the different MAP kinase inhibitors: U0126 and PD98059 prior to exposure to PAN. DMSO, used to reconstitute the inhibitors, was used as a control (Data shown was from U0126 inhibitor. A similar result was obtained with the PD98059 inhibitor).

IQGAP1 nuclear expression decreased significantly upon exposure to inhibitors (Figure 5A). Both inhibitors blocked the translocation of IQGAP1 into the nucleus (Figure 5B). The absence of detection of P-ERK expression upon Western blot in presence of the inhibitors confirmed the inhibition of ERK pathway activation.

These results suggest that nuclear translocation of IQGAP1 upon exposure to PAN requires ERK pathway activation and/or an efficient phosphorylation of ERK.

3.6. Interaction of IQGAP1 with chromatin

Chromatin immunoprecipitation assays were performed on control and PAN treated cell samples. Four different controls were used: PCR and primers templates, chromatin extract, rabbit IgG and Histone H3 antibody. PAN treatment resulted in a significant increase in the binding of IQGAP1 to chromatin. Interaction between IQGAP1 and chromatin was detected 90 min after exposure to PAN, as for the positive controls, chromatin extract and Histone H3 (Figure 6). Data were confirmed with a co-immunoprecipitation of Histone H3 on chromatin extract. The histone H3 co-immunoprecipitation allowed us to detect an interaction between IQGAP1 and the protein.

Cell survival assay was performed to investigate the potential role of IQGAP1 through its nuclear localization. As previously described [11], podocytes were transfected with IQGAP1 siRNA. 72 hours after transfection, IQGAP1 siRNA transfected podocytes were used for the assay in comparison to control cells (untransfected podocytes or Luciferase (Luc) siRNA transfected podocytes). PAN reduced the metabolic activity of podocytes compared with control podocytes. We have previously reported a defect of the cell motility in IQGAP1

siRNA transfected podocytes [11]. Addition of PAN did not change the cell migration phenotype (Data not shown). Proliferation properties remained unchanged (Supplementary material, Figure S4).

4. Discussion

In human podocytes treated with PAN, IQGAP1 translocates into the nucleus and there is a disruption of its interaction with podocyte specific proteins. The IQGAP1 nuclear translocation requires the ERK pathway and leads to IQGAP1 interaction with the chromatin.

PAN is a drug currently used to induce experimental nephrotic syndrome in rodent models but also used *in vitro* as an inducer of podocyte injury [35]. Liu et al. demonstrated the pivotal effect of PAN dose and PAN time exposure in terms of podocyte apoptosis. PAN effects on actin cytoskeleton and podocyte proteins such as podocin and nephrin have been already described: actin cytoskeleton change with podocin and nephrin redistribution [36]. In our work, PAN exposure did not induce differences of expression of the podocyte proteins (Nephrin and its phosphorylated form, podocalyxin and α-actinin 4) except for IQGAPs. Previous studies have reported a gap of a few days between the beginning of the injury and the decrease of protein expression upon exposure to PAN [30, 31]. PAN did not affect global IQGAP1 cell expression, although IQGAP1 localization in the different cell compartments changes with a cytoplasmic decrease and a nuclear increase, demonstrating nuclear translocation. Nuclear localization of IQGAPs has been previously reported in various cell lines [22, 37, 38]. We have demonstrated the nuclear expression of the two isoforms, IQGAP1 and 2, and interestingly we have observed a reverse expression pattern for IQGAP2 with PAN treatment causing a cytoplasmic accumulation of this protein. Although IQGAP isoforms have a notable homology of structure, their functions and/or tissue distribution are different [17, 39]. We may hypothesize that in human podocytes drugs such as PAN modify the

balance between IQGAP1 and IQGAP2 and therefore podocyte biology. Nuclear translocation of IQGAP1 was associated with a disruption of its interactions with specific podocyte proteins which may be relevant *in vivo* to the modification of the structure of the slit diaphragm and its associated proteins reported following PAN treatment. The conservation of the interaction between IQGAP1 and α-actinin-4 in our work suggests the conservation of the cytoskeletal structure over short time after PAN injury. After 24 hours of PAN treatment, Saleem et al. have described a stress fibre organization of actin cytoskeleton [33] with in some instances a granular distribution.

IQGAP1 is a scaffold protein serine and tyrosine-phosphorylated. Phosphorylation modulates its function. Other mechanisms are involved in IQGAP1 regulation, all influencing its role in biological processes. Serine-phosphorylation of IQGAP1 promotes neuronal outgrowth [40] and cytoskeleton regulation. In our PAN model, IQGAP1 phosphorylation is enhanced. Thus, we may hypothesize that PAN through IQGAP1 phosphorylation enhancement promotes its nuclear translocation and function.

With respect to IQGAP1 characteristics, we have explored different signaling pathways which may lead to a cytoplasmic-nuclear trafficking. ERK and β-catenin pathways are strong interacting partners of IQGAP1 that both have a known nuclear localization and function. We confirm an activation of the ERK pathway upon exposure to PAN, as reported by Liu et al. [32], and demonstrate that the activation of ERK pathway leads to a nuclear translocation of its phosphorylated form. IQGAP1 has been reported to be involved in ERK activation. IQGAP1 interacts with MEK 1/2 and ERK 1/2. The folding conformation of IQGAP1 allows the close contact of these interacting proteins and the activation of ERK 1/2 by MEK 1/2 [26, 27]. The phosphorylated form of ERK predominantly shuttles in the nuclei but a cytoplasmic pool is identified.

Our work for the first time suggests that the IQGAP1 nuclear translocation requires ERK pathway and its activation. Upon exposure to ERK inhibitors, the nuclear translocation induced by PAN is significantly reduced. ERK pathway may be the preponderant pathway involved in the IQGAP1 nucleo-cytoplasmic trafficking.

Johnson et al. have reported the nuclear shuttling of IQGAP1 independently of β-catenin pathway but regulated by GSK-3β [38]. Inhibition of GSK-3β induces an enhancement of IQGAP1 nuclear translocation. In our PAN model, neither activation of β-catenin pathway nor GSK-3β is associated with the nuclear IQGAP1 shuttle (Data not shown). We have also studied the Notch pathway due to the involvment of Notch activation in the development of glomerular disease [41]. Cell expression of Notch did not change in PAN treated cells compared to control cells (Data not shown).

Our work demonstrates the interaction between IQGAP1 and chromatin or Histone H3 in PAN treated cell conditions. Johnson et al. reported IQGAP1 shuttle during the cell cycle and its interaction with DNA replication complex [38]. The interaction type, whether direct or indirect, is still unknown and needs further studies. Histone H3 is an effector of ERK pathway which in turn mediates Histone H3 phosphorylation. The phosphorylated modification induces chromatin condensation, inhibition of cell proliferation and cell death [42]. IQGAP1, through its nuclear localization and therefore its interaction with the chromatin and Histone H3, may be a novel factor of post-translational modification which then modulates the cell survival. Podocyte survival is affected by PAN treatment, with a potential IQGAP1 involvement.

Figure 7 summarizes the PAN effect on podocyte and IQGAP1 biology.

In conclusion, PAN induced a nuclear translocation of IQGAP1 which required ERK pathway activation. This nuclear relocalization results in IQGAP1 interacting with the chromatin suggesting that IQGAP1 may be involved in podocyte gene transcription regulation.

5. Acknowledgements

CR was supported by a long-term fellowship from the ERA-EDTA (European Renal Association - European Dialysis and Transplant Association) and by grants from the Centre Hospitalier Universitaire de Bordeaux and the Société de Néphrologie. The advice and guidance of Jean Ripoche, INSERM U1026, Université de Bordeaux, F 33000, Bordeaux, France, is acknowledged.

6. Disclosure

All authors declared no competitive interests.

7. References

[1] M. Kestila, U. Lenkkeri, M. Mannikko, J. Lamerdin, P. McCready, H. Putaala, V. Ruotsalainen, T. Morita, M. Nissinen, R. Herva, C.E. Kashtan, L. Peltonen, C. Holmberg, A. Olsen, K. Tryggvason, Positionally cloned gene for a novel glomerular protein--nephrin--is mutated in congenital nephrotic syndrome, Mol Cell 1(4) (1998) 575-82.

[2] N. Boute, O. Gribouval, S. Roselli, F. Benessy, H. Lee, A. Fuchshuber, K. Dahan, M.C. Gubler, P. Niaudet, C. Antignac, NPHS2, encoding the glomerular protein podocin, is mutated in autosomal recessive steroid-resistant nephrotic syndrome, Nat Genet 24(4) (2000) 349-54.

[3] N.Y. Shih, J. Li, R. Cotran, P. Mundel, J.H. Miner, A.S. Shaw, CD2AP localizes to the slit diaphragm and binds to nephrin via a novel C-terminal domain, Am J Pathol 159(6) (2001) 2303-8.

[4] J.M. Kaplan, S.H. Kim, K.N. North, H. Rennke, L.A. Correia, H.Q. Tong, B.J. Mathis, J.C. Rodriguez-Perez, P.G. Allen, A.H. Beggs, M.R. Pollak, Mutations in ACTN4, encoding alpha-actinin-4, cause familial focal segmental glomerulosclerosis, Nat Genet 24(3) (2000) 251-6.

[5] B. Hinkes, R.C. Wiggins, R. Gbadegesin, C.N. Vlangos, D. Seelow, G. Nurnberg, P. Garg, R. Verma, H. Chaib, B.E. Hoskins, S. Ashraf, C. Becker, H.C. Hennies, M. Goyal, B.L. Wharram, A.D. Schachter, S. Mudumana, I. Drummond, D. Kerjaschki, R. Waldherr, A. Dietrich, F. Ozaltin, A. Bakkaloglu, R. Cleper, L. Basel-Vanagaite, M. Pohl, M. Griebel, A.N. Tsygin, A. Soylu, D. Muller, C.S. Sorli, T.D. Bunney, M. Katan, J. Liu, M. Attanasio, F. O'Toole J, K. Hasselbacher, B. Mucha, E.A. Otto, R. Airik, A. Kispert, G.G. Kelley, A.V. Smrcka, T. Gudermann, L.B. Holzman, P. Nurnberg, F. Hildebrandt, Positional cloning

uncovers mutations in PLCE1 responsible for a nephrotic syndrome variant that may be reversible, Nat Genet 38(12) (2006) 1397-405.
[6] M.P. Winn, P.J. Conlon, K.L. Lynn, M.K. Farrington, T. Creazzo, A.F. Hawkins, N. Daskalakis, S.Y. Kwan, S. Ebersviller, J.L. Burchette, M.A. Pericak-Vance, D.N. Howell, J.M. Vance, P.B. Rosenberg, A mutation in the TRPC6 cation channel causes familial focal segmental glomerulosclerosis, Science 308(5729) (2005) 1801-4.
[7] E.J. Brown, J.S. Schlondorff, D.J. Becker, H. Tsukaguchi, S.J. Tonna, A.L. Uscinski, H.N. Higgs, J.M. Henderson, M.R. Pollak, Mutations in the formin gene INF2 cause focal segmental glomerulosclerosis, Nat Genet 42(1) (2010) 72-6.
[8] J. Dantal, E. Bigot, W. Bogers, A. Testa, F. Kriaa, Y. Jacques, B. Hurault de Ligny, P. Niaudet, B. Charpentier, J.P. Soulillou, Effect of plasma protein adsorption on protein excretion in kidney-transplant recipients with recurrent nephrotic syndrome, N Engl J Med 330(1) (1994) 7-14.
[9] X.L. Liu, P. Kilpelainen, U. Hellman, Y. Sun, J. Wartiovaara, E. Morgunova, T. Pikkarainen, K. Yan, A.P. Jonsson, K. Tryggvason, Characterization of the interactions of the nephrin intracellular domain, Febs J 272(1) (2005) 228-43.
[10] S. Lehtonen, J.J. Ryan, K. Kudlicka, N. Iino, H. Zhou, M.G. Farquhar, Cell junction-associated proteins IQGAP1, MAGI-2, CASK, spectrins, and alpha-actinin are components of the nephrin multiprotein complex, Proc Natl Acad Sci U S A 102(28) (2005) 9814-9.
[11] C. Rigothier, P. Auguste, G.I. Welsh, S. Lepreux, C. Deminiere, P.W. Mathieson, M.A. Saleem, J. Ripoche, C. Combe, IQGAP1 Interacts with Components of the Slit Diaphragm Complex in Podocytes and Is Involved in Podocyte Migration and Permeability In Vitro, PLoS One 7(5) (2012) e37695.
[12] T. Watanabe, J. Noritake, M. Kakeno, T. Matsui, T. Harada, S. Wang, N. Itoh, K. Sato, K. Matsuzawa, A. Iwamatsu, N. Galjart, K. Kaibuchi, Phosphorylation of CLASP2 by GSK-3beta regulates its interaction with IQGAP1, EB1 and microtubules, J Cell Sci 122(Pt 16) (2009) 2969-79.
[13] M. Fukata, T. Watanabe, J. Noritake, M. Nakagawa, M. Yamaga, S. Kuroda, Y. Matsuura, A. Iwamatsu, F. Perez, K. Kaibuchi, Rac1 and Cdc42 capture microtubules through IQGAP1 and CLIP-170, Cell 109(7) (2002) 873-85.
[14] Y. Liu, W. Liang, Y. Yang, Y. Pan, Q. Yang, X. Chen, P.C. Singhal, G. Ding, IQGAP1 regulates actin cytoskeleton organization in podocytes through interaction with nephrin, Cell Signal 27(4) (2015) 867-77.
[15] L. Weissbach, J. Settleman, M.F. Kalady, A.J. Snijders, A.E. Murthy, Y.X. Yan, A. Bernards, Identification of a human rasGAP-related protein containing calmodulin-binding motifs, J Biol Chem 269(32) (1994) 20517-21.
[16] S. Brill, S. Li, C.W. Lyman, D.M. Church, J.J. Wasmuth, L. Weissbach, A. Bernards, A.J. Snijders, The Ras GTPase-activating-protein-related human protein IQGAP2 harbors a potential actin binding domain and interacts with calmodulin and Rho family GTPases, Mol Cell Biol 16(9) (1996) 4869-78.
[17] S. Wang, T. Watanabe, J. Noritake, M. Fukata, T. Yoshimura, N. Itoh, T. Harada, M. Nakagawa, Y. Matsuura, N. Arimura, K. Kaibuchi, IQGAP3, a novel effector of Rac1 and Cdc42, regulates neurite outgrowth, J Cell Sci 120(Pt 4) (2007) 567-77.
[18] M.J. Hart, M.G. Callow, B. Souza, P. Polakis, IQGAP1, a calmodulin-binding protein with a rasGAP-related domain, is a potential effector for cdc42Hs, Embo J 15(12) (1996) 2997-3005.
[19] J.L. Joyal, R.S. Annan, Y.D. Ho, M.E. Huddleston, S.A. Carr, M.J. Hart, D.B. Sacks, Calmodulin modulates the interaction between IQGAP1 and Cdc42. Identification of IQGAP1 by nanoelectrospray tandem mass spectrometry, J Biol Chem 272(24) (1997) 15419-25.

[20] S. Kuroda, M. Fukata, K. Kobayashi, M. Nakafuku, N. Nomura, A. Iwamatsu, K. Kaibuchi, Identification of IQGAP as a putative target for the small GTPases, Cdc42 and Rac1, J Biol Chem 271(38) (1996) 23363-7.
[21] Z. Li, S.H. Kim, J.M. Higgins, M.B. Brenner, D.B. Sacks, IQGAP1 and calmodulin modulate E-cadherin function, J Biol Chem 274(53) (1999) 37885-92.
[22] S. Kuroda, M. Fukata, M. Nakagawa, K. Fujii, T. Nakamura, T. Ookubo, I. Izawa, T. Nagase, N. Nomura, H. Tani, I. Shoji, Y. Matsuura, S. Yonehara, K. Kaibuchi, Role of IQGAP1, a target of the small GTPases Cdc42 and Rac1, in regulation of E-cadherin-mediated cell-cell adhesion, Science 281(5378) (1998) 832-5.
[23] E.N. Rittmeyer, S. Daniel, S.C. Hsu, M.A. Osman, A dual role for IQGAP1 in regulating exocytosis, J Cell Sci 121(Pt 3) (2008) 391-403.
[24] M.W. Briggs, Z. Li, D.B. Sacks, IQGAP1-mediated stimulation of transcriptional co-activation by beta-catenin is modulated by calmodulin, J Biol Chem 277(9) (2002) 7453-65.
[25] A.T. Willingham, A.P. Orth, S. Batalov, E.C. Peters, B.G. Wen, P. Aza-Blanc, J.B. Hogenesch, P.G. Schultz, A strategy for probing the function of noncoding RNAs finds a repressor of NFAT, Science 309(5740) (2005) 1570-3.
[26] M. Roy, Z. Li, D.B. Sacks, IQGAP1 binds ERK2 and modulates its activity, J Biol Chem 279(17) (2004) 17329-37.
[27] M. Roy, Z. Li, D.B. Sacks, IQGAP1 is a scaffold for mitogen-activated protein kinase signaling, Mol Cell Biol 25(18) (2005) 7940-52.
[28] B.S. Kaplan, L. Renaud, K.N. Drummond, Effects of aminonucleoside, daunomycin, and adriamycin on carbon oxidation by glomeruli, Lab Invest 34(2) (1976) 174-8.
[29] J.P. Caulfield, J.J. Reid, M.G. Farquhar, Alterations of the glomerular epithelium in acute aminonucleoside nephrosis. Evidence for formation of occluding junctions and epithelial cell detachment, Lab Invest 34(1) (1976) 43-59.
[30] F. Duner, K. Lindstrom, K. Hultenby, J. Hulkko, J. Patrakka, K. Tryggvason, B. Haraldsson, A. Wernerson, E. Pettersson, Permeability, ultrastructural changes, and distribution of novel proteins in the glomerular barrier in early puromycin aminonucleoside nephrosis, Nephron Exp Nephrol 116(2) (2010) e42-52.
[31] N. Guan, J. Ding, J. Deng, J. Zhang, J. Yang, Key molecular events in puromycin aminonucleoside nephrosis rats, Pathol Int 54(9) (2004) 703-11.
[32] S. Liu, J. Ding, Q. Fan, H. Zhang, The activation of extracellular signal-regulated kinase is responsible for podocyte injury, Mol Biol Rep 37(5) (2010) 2477-84.
[33] M.A. Saleem, M.J. O'Hare, J. Reiser, R.J. Coward, C.D. Inward, T. Farren, C.Y. Xing, L. Ni, P.W. Mathieson, P. Mundel, A conditionally immortalized human podocyte cell line demonstrating nephrin and podocin expression, J Am Soc Nephrol 13(3) (2002) 630-8.
[34] R.J. Coward, R.R. Foster, D. Patton, L. Ni, R. Lennon, D.O. Bates, S.J. Harper, P.W. Mathieson, M.A. Saleem, Nephrotic plasma alters slit diaphragm-dependent signaling and translocates nephrin, Podocin, and CD2 associated protein in cultured human podocytes, J Am Soc Nephrol 16(3) (2005) 629-37.
[35] J.W. Pippin, P.T. Brinkkoetter, F.C. Cormack-Aboud, R.V. Durvasula, P.V. Hauser, J. Kowalewska, R.D. Krofft, C.M. Logar, C.B. Marshall, T. Ohse, S.J. Shankland, Inducible rodent models of acquired podocyte diseases, Am J Physiol Renal Physiol 296(2) (2009) F213-29.
[36] M.A. Saleem, L. Ni, I. Witherden, K. Tryggvason, V. Ruotsalainen, P. Mundel, P.W. Mathieson, Co-localization of nephrin, podocin, and the actin cytoskeleton: evidence for a role in podocyte foot process formation, Am J Pathol 161(4) (2002) 1459-66.
[37] C.S. Chew, C.T. Okamoto, X. Chen, H.Y. Qin, IQGAPs are differentially expressed and regulated in polarized gastric epithelial cells, Am J Physiol Gastrointest Liver Physiol 288(2) (2005) G376-87.

[38] M. Johnson, M. Sharma, M.G. Brocardo, B.R. Henderson, IQGAP1 translocates to the nucleus in early S-phase and contributes to cell cycle progression after DNA replication arrest, Int J Biochem Cell Biol 43(1) (2011) 65-73.
[39] M.W. Briggs, D.B. Sacks, IQGAP proteins are integral components of cytoskeletal regulation, EMBO Rep 4(6) (2003) 571-4.
[40] Z. Li, D.E. McNulty, K.J. Marler, L. Lim, C. Hall, R.S. Annan, D.B. Sacks, IQGAP1 promotes neurite outgrowth in a phosphorylation-dependent manner, J Biol Chem 280(14) (2005) 13871-8.
[41] T. Niranjan, B. Bielesz, A. Gruenwald, M.P. Ponda, J.B. Kopp, D.B. Thomas, K. Susztak, The Notch pathway in podocytes plays a role in the development of glomerular disease, Nat Med 14(3) (2008) 290-8.
[42] K. Tikoo, S.S. Lau, T.J. Monks, Histone H3 phosphorylation is coupled to poly-(ADP-ribosylation) during reactive oxygen species-induced cell death in renal proximal tubular epithelial cells, Mol Pharmacol 60(2) (2001) 394-402.

8. Figure legends

Figure 1

IQGAP1 localization and expression in PAN treated podocytes.

A. IQGAP1 (green labelling) in control condition was expressed at the cell membrane and cell-cell contacts (Plain arrows). In PAN treated podocytes, cell redistribution was observed with a predominant nuclear localization (Dashed arrows), with persistent usual membranous localization. DAPI staining (blue labelling) confirmed nuclear merge.

B. Western blot analyses for IQGAP1 and β-actin were performed on cytoplasmic and nuclear extracts at different times of exposure to PAN: untreated podocytes (control), 60 (PAN 60) and 90 minutes (PAN 90). Laminin γ1 and lamin A/C were used as controls of the selective extraction and absence of contamination between the 2 cell fractions. Laminin γ1 and lamin A/C were exclusively and respectively cytoplasmic and nuclear proteins. The blot is representative of eight independent experiments.

C. IQGAP1 expression on both cell compartment was quantified with the Biorad® software. In order to appreciate IQGAP1 intracellular trafficking, cytoplasmic expression was reported to nuclear expression. The ratio demonstrated the nuclear translocation of the IQGAP1 protein. Asterisk significative difference with control podocytes: ⋆ $p<0.05$, ⋆⋆ $p<0.01$, Repeated measures ANOVA. The blot is representative of eight independent experiments.

Figure 2

IQGAP2 expression in PAN treated podocytes.

A. Western blot analyses of IQGAP2 expression were performed on cytoplasmic and nuclear extracts. IQGAP2 expression was indexed to β-actin expression. The blot is representative of eight experiments. Control: untreated podocytes, PAN 90: podocytes exposed 90 min to PAN.

B. Cytoplasmic and nuclear expression of IQGAP2 was plotted by densitometry, reported to β-actin expression. Ratio between cytoplasm and nuclei expressions allowed us to appreciate the shuttle of IQGAP2 between the two cell compartments. The cytoplasmic accumulation was significant ($p<0.05$, Paired t-test).

Figure 3

Expression of podocyte proteins and their interaction with IQGAP1 upon exposure to PAN.

A. Western blot analyses were performed on total, cytoplasmic and nuclear extracts at different times of exposure to PAN. Expression of nephrin, phosphorylated nephrinY1176, podocalyxin and α-actinin-4 was detected. The blot is representative of five independent experiments. Control: untreated podocytes, PAN 90: podocytes exposed for 90 min to PAN.

B. Quantification of the expression of podocyte proteins on cytoplasmic and nuclear cell extracts. No differences were detected (n=5, Wilcoxon's test).

C. IQGAP1 co-immunoprecipitations with the different podocyte proteins were performed on cytoplasmic extracts. IQGAP1 interacted with the different proteins. Protein A/G agarose beads (Prot A/G) in presence of cytoplasmic lysate were used as negative control. Control: untreated podocytes, PAN 90: podocytes exposed 90 min to PAN (n=5).

D. Interactions between IQGAP1 and podocyte proteins were quantified by densitometry. For each interaction, the value of the interacting protein was reported to the corresponding

IQGAP1 value. PAN induced a significant decrease of the interaction between IQGAP1 and podocyte proteins (n=5, $p<0.05$, Paired t-test).

Figure 4

Activation of ERK pathway.

A. Western blot analyses of the expression of ERK and P-ERK were performed on total, cytoplasmic and nuclear extracts at different times of exposure to PAN. The blot was representative of six independent experiments. Control: untreated podocytes, PAN 90: podocytes exposed 90 min to PAN.

B. Expression of ERK and P-ERK on total, cytoplasmic and nuclear cell extracts was quantified with the Biorad® software (n=6, ✶ $p<0.05$, ✶✶ $p<0.01$,Paired t-test).

C. Evaluation of the phosphorylation degree of ERK and its cell shuttle. We evaluated ERK phosphorylation plotting the expression of P-ERK to ERK, on cytoplasmic and nuclear extracts. Ratio between the cytoplasmic and nuclear ERK phosphorylation demonstrate the nuclear shuttle of P-ERK (n=6, ✶ $p<0.05$, ✶✶ $p<0.01$, Paired t-test).

D. IQGAP1 co-immunoprecipitations with ERK and P-ERK were performed on cytoplasmic and nuclear extracts. Protein A/G agarose beads (Prot A/G) were used as control. Control: untreated podocytes, PAN 90: podocytes exposed 90 min to PAN (n=5).

E. Interaction between IQGAP1 and nuclear P-ERK increased significantly and was confirmed by densitometry data (n=5, ✶ $p<0.05$, Paired t-test).

Figure 5

Effect of ERK pathway inhibitor on IQGAP1 translocation.

A. Western blot analyses of IQGAP1 expression were done on cytoplasmic and nuclear extracts. Inhibition of ERK pathway was confirmed by P-ERK blotting. Six different

conditions were studied: 1-control, 2-Control+DMSO, 3-Control+Inhibitor (here U0126 but similar results were obtained with PD98059), 4-PAN90, 5-PAN90+DMSO, 6-PAN90+Inhibitor. The blot is representative of 7 independent experiments for U0126 and PD98059.

B. Cytoplasmic IQGAP1 expression was plotted in each condition and reported to nuclear IQGAP1 expression, after quantification by Biorad® software. The ratio is the result of the nucleocytoplasmic trafficking (n=7 per inhibitor, ⋆ $p<0.05$, ⋆⋆ $p<0.01$, Paired t-test).

Figure 6

Chromatin immunoprecipitation assay.

A. Interaction between IQGAP1 and the chromatin 90 min upon exposure to PAN, explored by CHIP assay. RPL30 PCR product is at 150bp. Four controls were used, two positives: chromatin and histone H3 and two negatives: rabbit IgG and the PCR/primers template.

B. Co-immunoprecipitation confirmed the interaction and clarified the potential site: IQGAP1 interacted with the Histone H3 in chromatin extracts. IgG: rabbit IgG, MW: molecular weight with 250 and 150 kDa markers, Input: chromatin extract, H3: Histone H3.

Figure 7

Schematic representation of the podocyte and IQGAP1 biology modification occurring during PAN exposure

Table 1: List of the different antibodies (IF = Immunofluorescence, WB = Western blot, IP = Immunoprecipitation).

Primary antibodies	**Source**	**Applications**	**Dilution**	**Origin**
IQGAP1	Mouse mAb, clone AF4	IF	IF: 1/100	Upstate
	Rabbit pAb, H-109	IF, WB, IP	WB: 1/1000	Santa Cruz
	Mouse mAb	WB	IP: 3 µg	BD biosciences
β-actin	Mouse mAb	WB	WB: 1/10000	Sigma-Aldrich
Lamin A/B	Mouse mAb, ab8984	WB	WB: 1/1000	Abcam
Laminin γ1	Goat mAb, C-20	WB	WB: 1/1000	Santa Cruz
IQGAP2	Mouse mAb,	WB	WB: 1/500	Santa Cruz
Nephrin	Rabbit pAb, H-300	WB	WB: 1/1000	Santa Cruz
Phosphorylated nephrin Y1176	Rabbit pAb	WB	WB: 1/1000	Gift
Podocalyxin	Mouse mAb	WB	WB: 1/1000	Pr Ronco
α-actinin-4	Rabbit pAb	WB	WB: 1/1000	Alexis
ERK 1/2 (p44/42 MAPK)	Rabbit pAb	WB	WB: 1/1000	Cell signaling
Phospho-ERK 1/2 (Phospho-p44/42 MAPK)	Rabbit pAb	WB	WB: 1/1000	Cell signaling
Histone H3	Rabbit mAb	IP	IP: 10 µl	Cell signaling
Secondary antibodies		**Applications**	**Dilution**	**Origin**
Alexa Fluor 488 Goat anti rabbit		IF	1/200	Molecular Probes
Alexa Fluor 488 Goat anti mouse		IF	1/200	Molecular Probes
Goat anti rabbit HRP conjugated		WB	1/10000	GE Healthcare
Goat anti mouse HRP conjugated		WB	1/10000	GE Healthcare
Donkey anti goat HRP conjugated		WB	1/10000	Santa Cruz

Figure(s)

Click here to download high resolution image

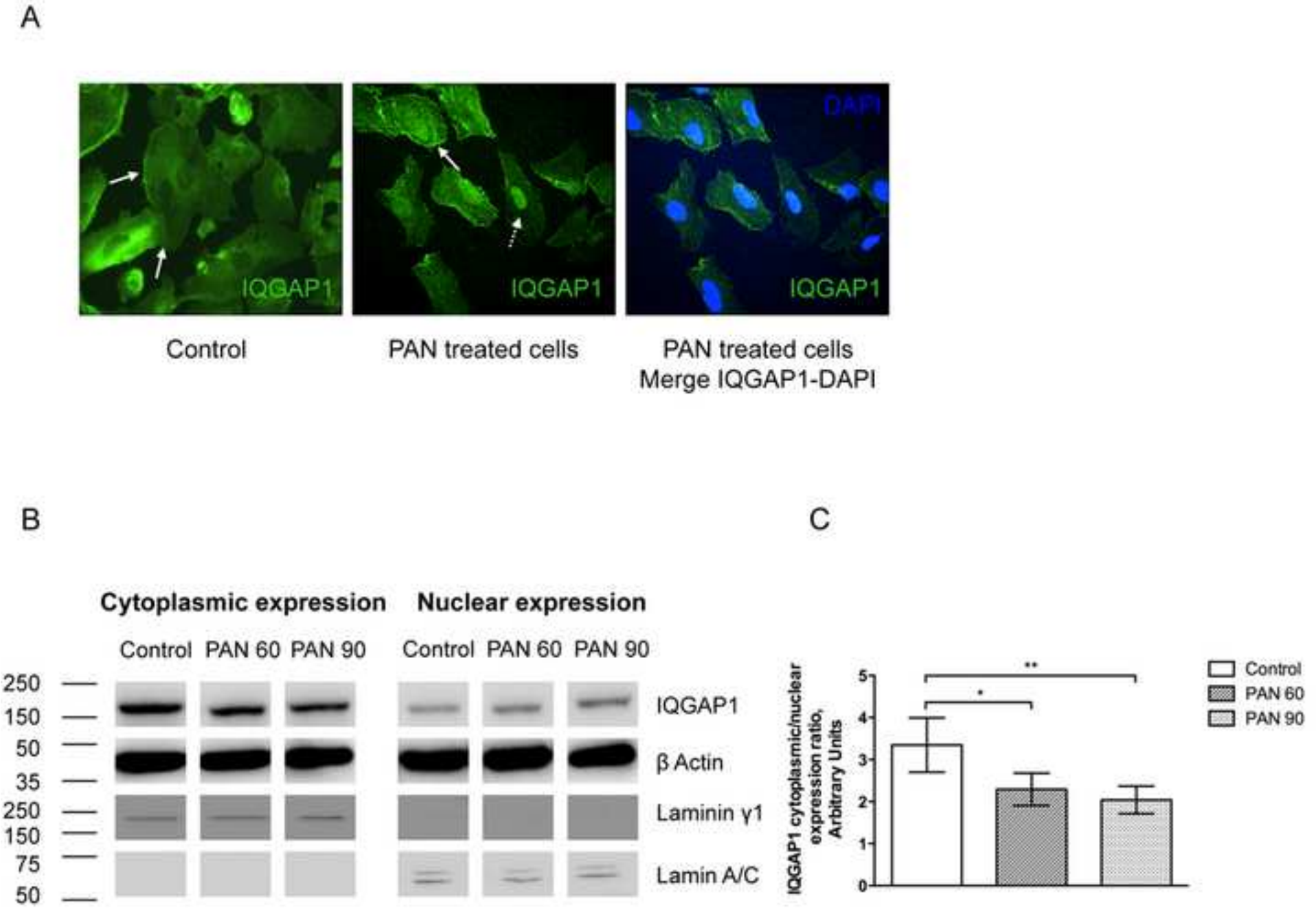

Figure(s)

Click here to download high resolution image

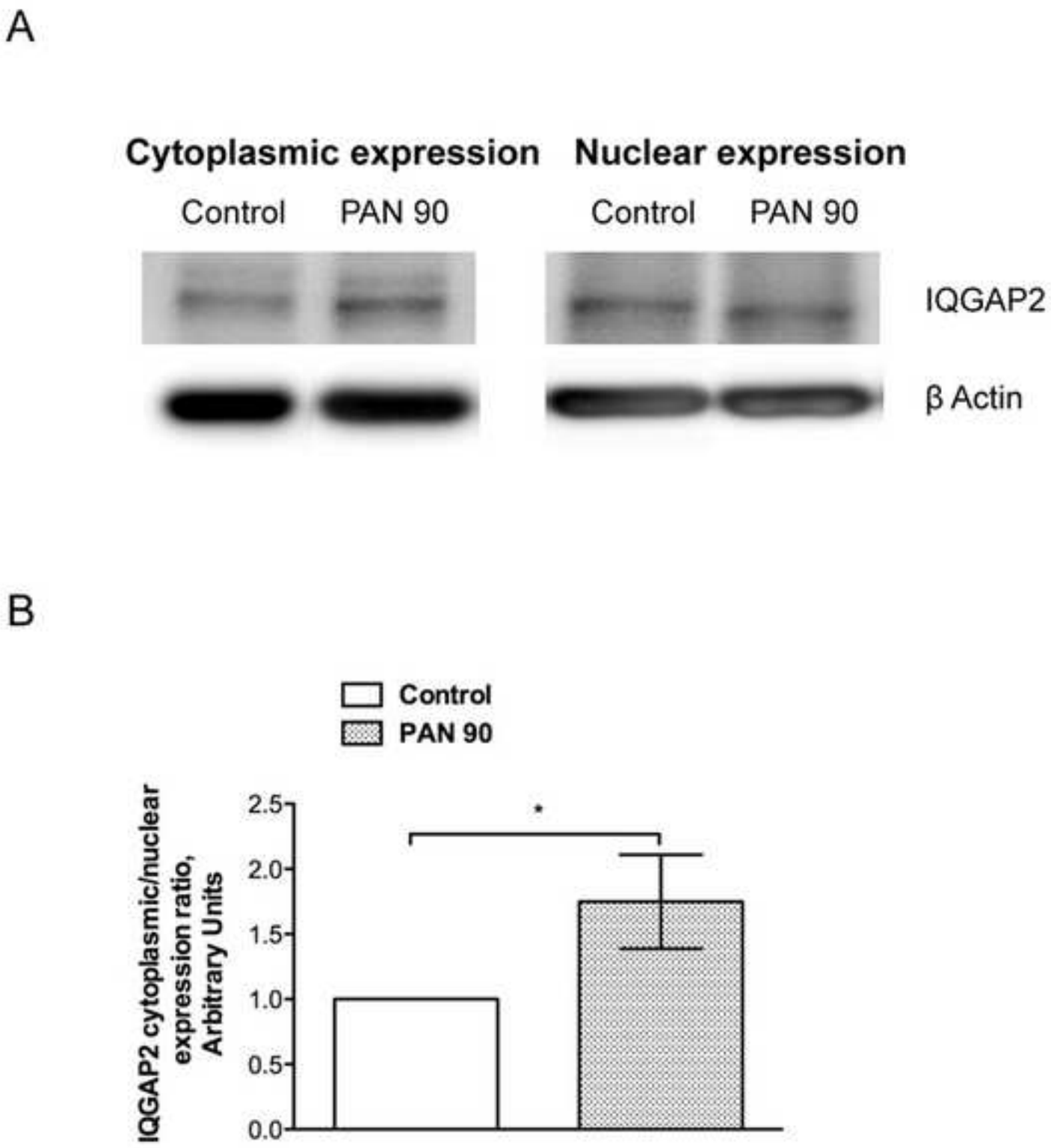

Figure(s)

Click here to download high resolution image

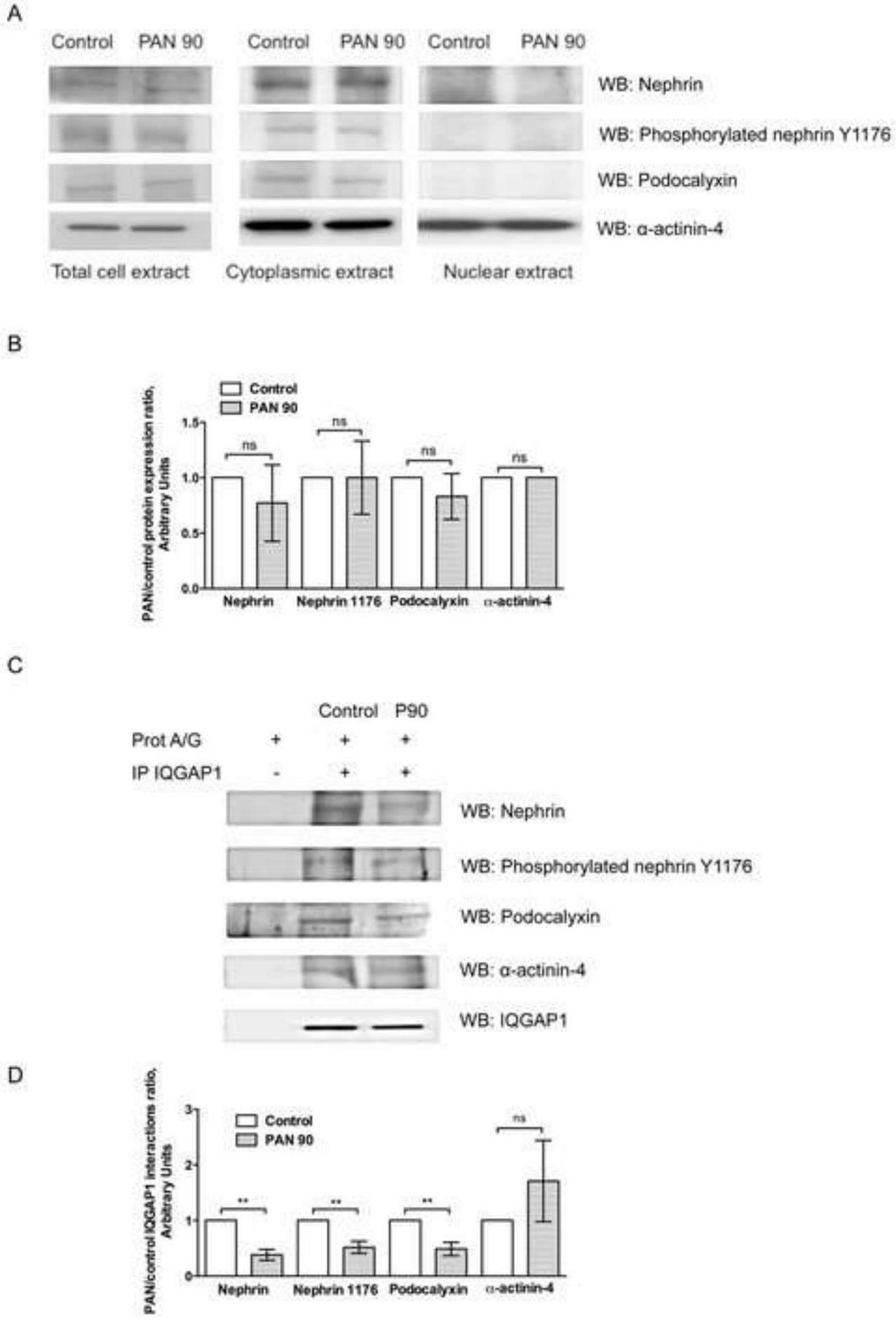

Figure(s)

Click here to download high resolution image

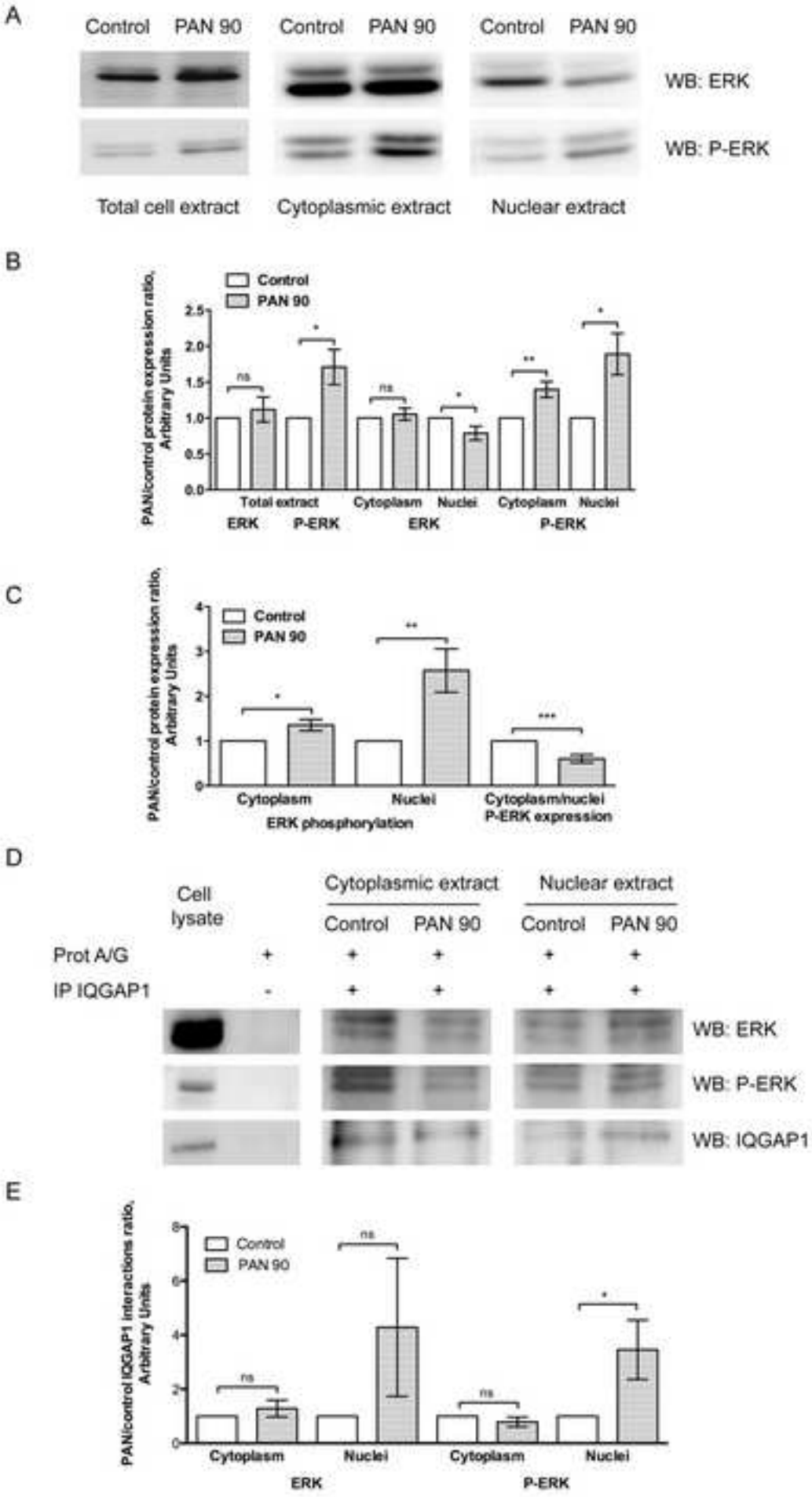

Figure(s)

Click here to download high resolution image

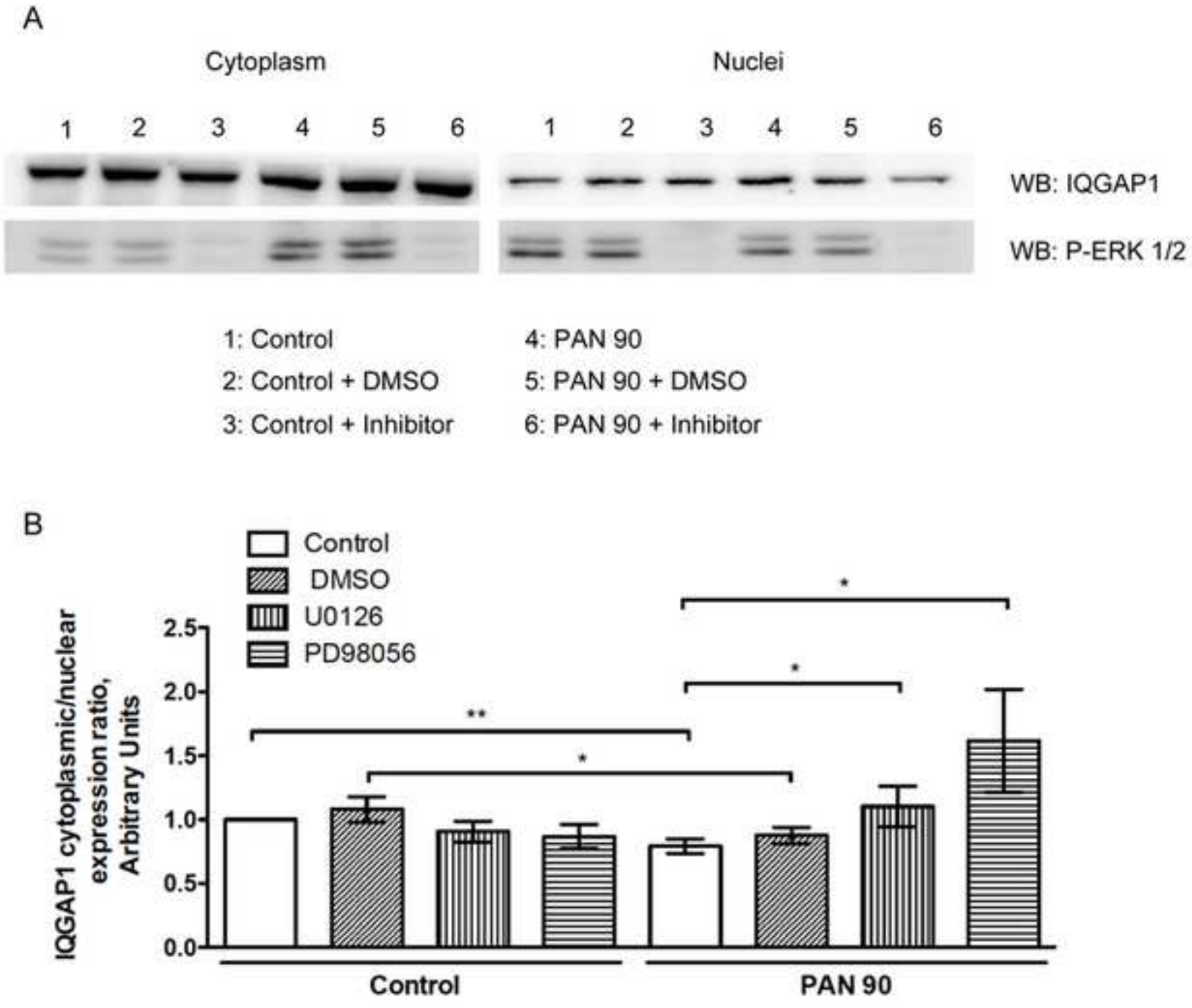

Figure(s)

Click here to download high resolution image

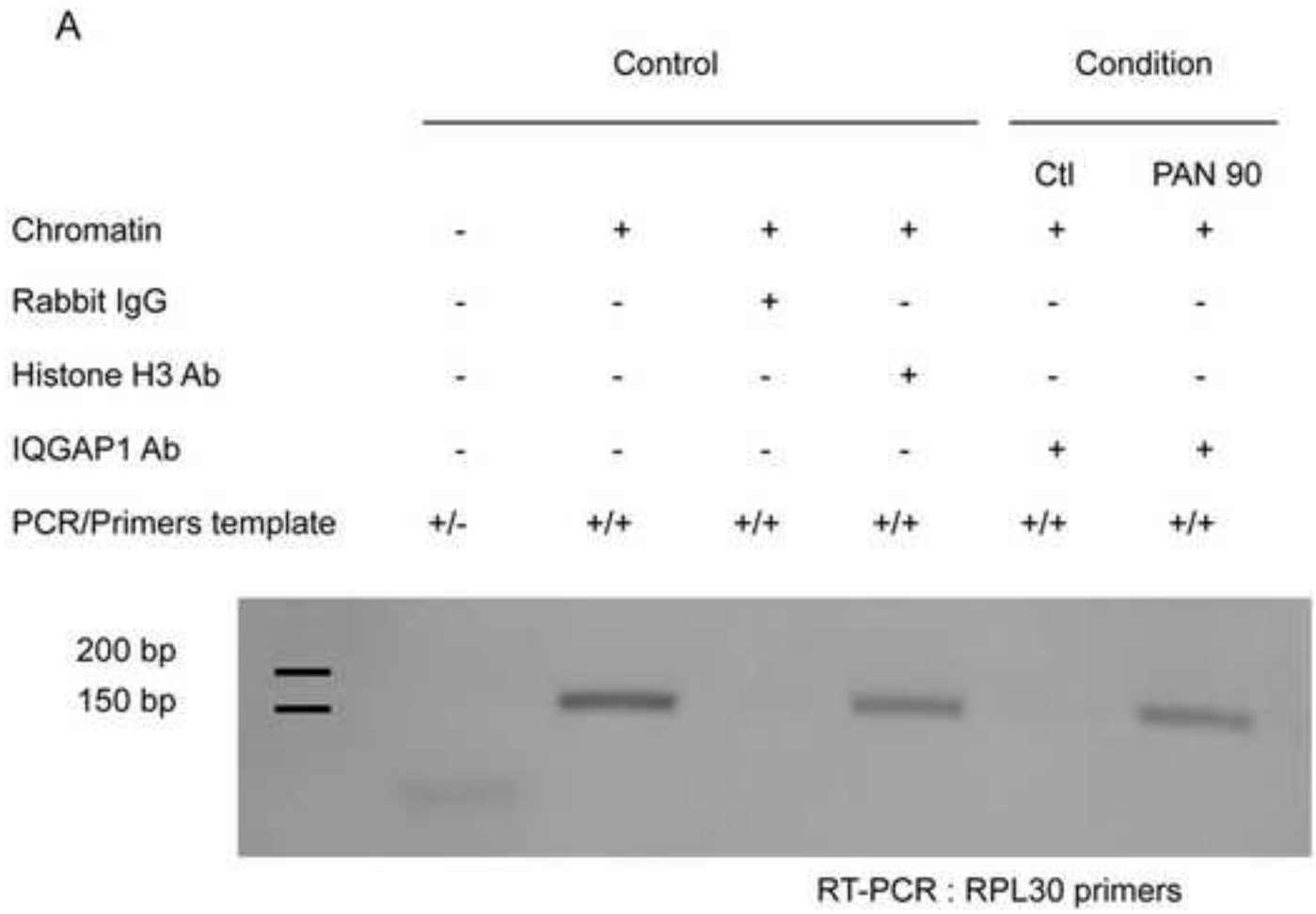

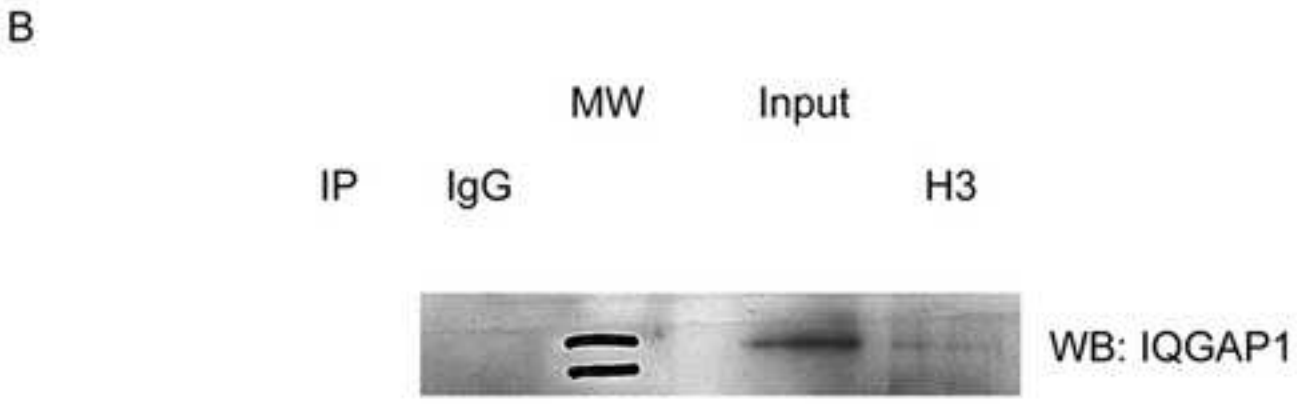

Figure(s)

Click here to download high resolution image

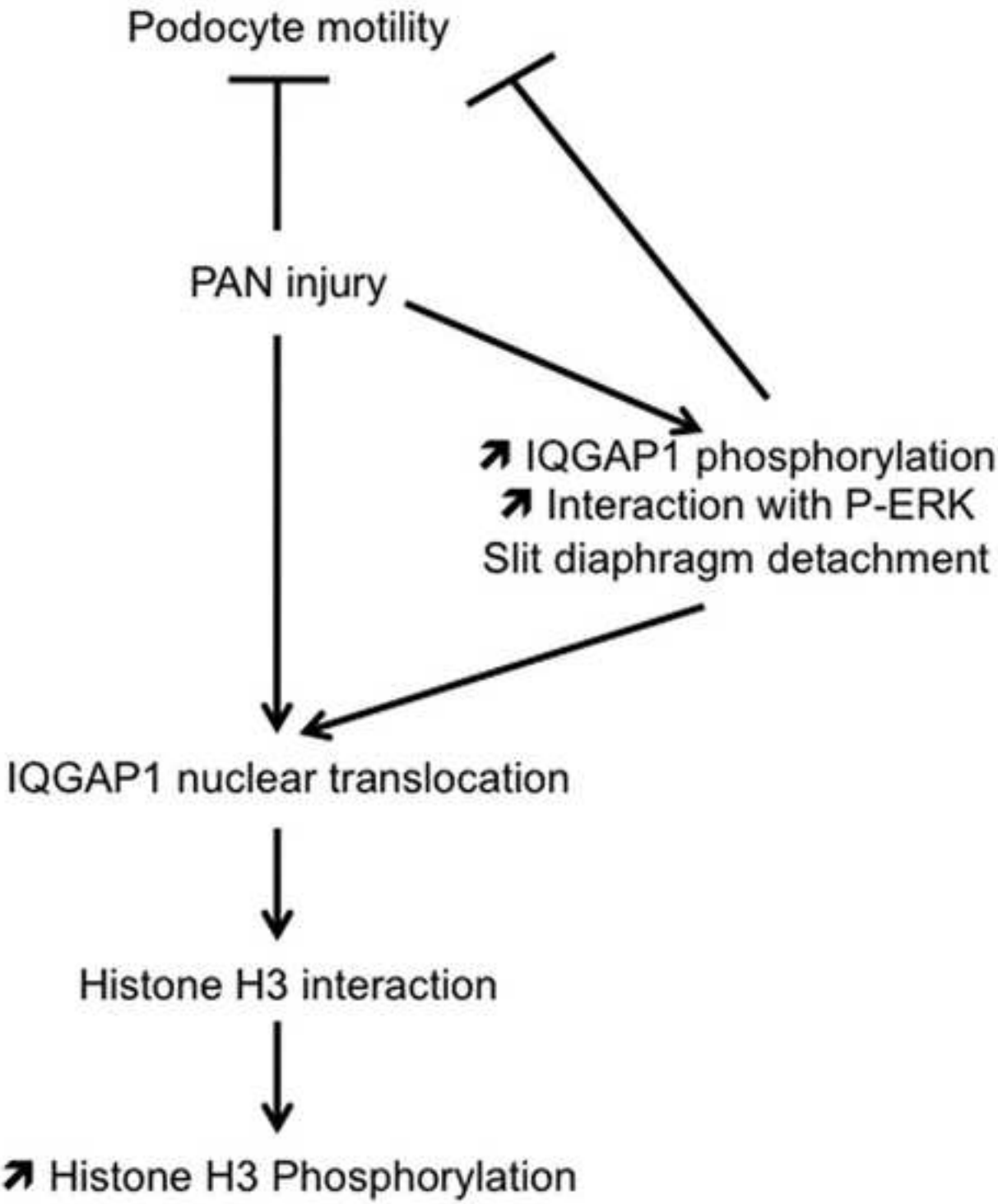

Supplementary Material

Click here to download Supplementary Material: R1 Supplementary material.doc